

## Electrochemical Characterization of Mesoporous NiCo<sub>2</sub>O<sub>4</sub> Nanocomposites Synthesized by a Xerogel Route

Ni WANG<sup>a</sup>, Meng-Qi YAO<sup>b</sup>, Qian ZHANG<sup>c</sup> and Wen-Cheng HU<sup>d, \*</sup>

State Key Laboratory of Electronic Thin Films and Integrated Devices, University of Electronic Science & Technology of China, Chengdu 610054, P. R. China

<sup>a</sup>niwang1226@gmail.com, <sup>b</sup>mengqiyao@hotmail.com, <sup>c</sup>zhangqianba@163.com, <sup>d</sup>huwc@uestc.edu.cn

\* Corresponding author: huwc@uestc.edu.cn

**Keywords:** Mesoporous NiCo<sub>2</sub>O<sub>4</sub> nanocomposite, Specific capacity, Battery-type electrode.

**Abstract.** Mesoporous NiCo<sub>2</sub>O<sub>4</sub> nanocomposites have been successfully synthesized by a xerogel route followed by heat-treatment process using propylene oxide as a gelation agent. The prepared materials are characterized by X-ray diffraction, FESEM, HRTEM and N<sub>2</sub> adsorption/desorption. The results suggest the NiCo<sub>2</sub>O<sub>4</sub> nanocomposites possessing a high specific surface area of 134 m<sup>2</sup> g<sup>-1</sup> and a mesoporous structure. Cyclic voltammetry (CV) and galvanostatic technique are employed to evaluate the mesoporous NiCo<sub>2</sub>O<sub>4</sub> electrode in 7 M KOH aqueous solution. A maximum specific capacity of 392 C g<sup>-1</sup> is calculated on the basis of the galvanostatic discharge curve at a current density of 1 A g<sup>-1</sup>, implying excellent performance for a battery-type electrode.

### Introduction

The capacity of an energy device is closely related to the conductivity, specific surface area and pore structure of an electrode material [1-5]. Recently, NiCo<sub>2</sub>O<sub>4</sub>, a binary transition metal oxide, has been demonstrated that it possesses the better conductivity than that of the individual nickel oxide or cobalt oxide [6-8]. Obviously, this meets the practical application of electro-active materials with excellent electrochemical properties.

Mesoporous materials with fine nanostructure usually have a high surface area, and appropriate pore size distribution [9,10], which is beneficial to the improvement of capacity, because the fast Faradaic reaction mostly occurs at the electrode/electrolyte interface. Many methods have been used to synthesize mesoporous structure NiCo<sub>2</sub>O<sub>4</sub>, such as microwave synthesis [11], KIT-6 hard template [12], hydrothermal reaction [13], sol-gel route [14], electrochemical deposition [15], etc. In the present work, we suggest a xerogel route to prepare the mesoporous NiCo<sub>2</sub>O<sub>4</sub> nanocomposites with the excellent electrochemical properties for the potential application in electrochemical energy conversion devices.

### Experimental

#### Material Synthesis

Analytically pure nickel (II) nitrate hexahydrate (Ni(NO<sub>3</sub>)<sub>2</sub>•6H<sub>2</sub>O) cobaltous nitrate hexahydrate (Co(NO<sub>3</sub>)<sub>2</sub>•6H<sub>2</sub>O) with a mole ratio of 1:2 were dissolved in ethyl alcohol to obtain a clear solution with a Ni+Co concentration of 0.3M. Propylene oxide (propylene oxide/(Ni+Co)=11), as a gelation agent, was rapidly added to the above solution under magnetic stirring, and a rigid dark-violet gel was formed within several minutes. Acetonitrile was employed to displace the solvents (ethyl alcohol and water) existed in the aged gel for three times. Acetonitrile was thoroughly volatilized in a vacuum drying oven at 100 °C to prepare the xerogel. The xerogel was annealed at 320 °C for 20min with a heating rate of 3 °C per minute to finish the synthesis of mesoporous NiCo<sub>2</sub>O<sub>4</sub> nanocomposites.

## Material Characterization

X-ray diffraction (XRD, Rigaku Co., Japan) was employed to characterize the crystal structures, and field-emission scanning electron microscopy (Inspect F, FEI Co., U.S.) and high-resolution transmission electron microscopy (HRTEM; Libra 200FE, Germany) were used to investigate the micro-morphologies of the mesoporous  $\text{NiCo}_2\text{O}_4$  nanocomposites. The surface area and pore size distributions were derived from the calculated results of the BET equation and the BJH method based on the  $\text{N}_2$  adsorption and desorption experiments operated on a JW-BK112 Surface Characterization Analyzer (Beijing JWGB Sci & Tech Co., China).

The mesoporous  $\text{NiCo}_2\text{O}_4$  nanocomposites mixed with 10 wt% acetylene black and 10 wt% polyvinylidene fluoride were pressed onto carbon felt with an approximate mass loading of  $3\text{ mg cm}^{-2}$  to prepare the working electrode for evaluation of the electrochemical characteristics of mesoporous  $\text{NiCo}_2\text{O}_4$  nanocomposites. A typical three-electrode cell, equipped with an Hg/HgO reference electrode and a Pt plate electrode counter, and using 7 M KOH aqueous solution as electrolyte, was measured in an electrochemical workstation (CHI660D, Chenhua) to record the results of cyclic voltammetry (CV) and electrochemical impedance spectroscopy (EIS). Galvanostatic charge–discharge was carried out in a Lanhe battery testing system.

## Results and Discussion

A representative XRD pattern of the mesoporous  $\text{NiCo}_2\text{O}_4$  nanocomposite annealed at  $320\text{ }^\circ\text{C}$  for 20 min given in Fig. 1. It can be noted that peaks located at  $31.1\text{ }^\circ$ ,  $36.5\text{ }^\circ$ ,  $44.5\text{ }^\circ$ ,  $55.4\text{ }^\circ$ ,  $59.2\text{ }^\circ$  and  $66.1\text{ }^\circ$  belong to  $\text{NiCo}_2\text{O}_4$  (PCPDF No.73-1702). The X-ray peak intensity indicates the inferior crystallinity of the sample. A further analysis of the XRD pattern reveals that a peak at  $43.1\text{ }^\circ$  can be indexed to the (200) plane reflection of the cubic NiO (PCPDF No. 73-1519), implying the formation of the NiO secondary phase in  $\text{NiCo}_2\text{O}_4$  nanocomposite.

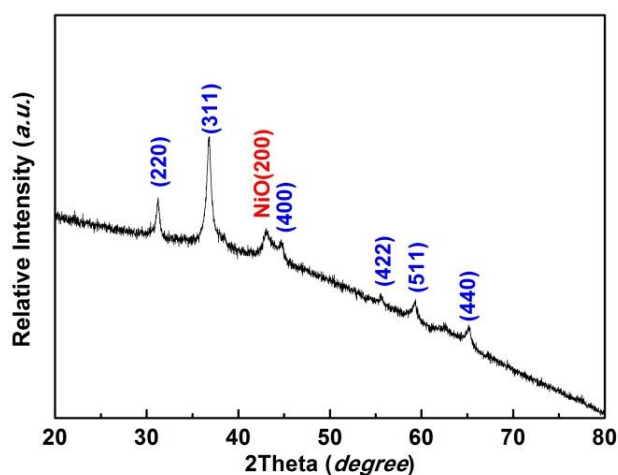


Fig. 1 XRD pattern of the mesoporous  $\text{NiCo}_2\text{O}_4$  nanocomposite

The SEM micrograph of the  $\text{NiCo}_2\text{O}_4$  nanocomposite is shown in Fig. 2. The xerogel particles are the agglomerates of very fine particles with different shapes, and many pores with different sizes are formed among the fine particles exhibiting a 3D continuous structure. To get farther understanding of microstructure, a transmission electron microscope was used to investigate the mesoporous  $\text{NiCo}_2\text{O}_4$  nanocomposite (inset of Fig. 2). The HRTEM image delivers well-defined lattice fringes within a small area, suggesting many tiny

and inferior crystalline grains involved in the mesoporous  $\text{NiCo}_2\text{O}_4$  nanocomposite, which agrees with the result of XRD.

Fig. 3 exhibits  $\text{N}_2$  adsorption–desorption isotherms of  $\text{NiCo}_2\text{O}_4$  nanocomposite. Obviously, the isotherms belong to type IV[16]. It can be observed that a hysteresis loop of type H3 presents in the relative pressure range from 0.65 to 0.96, revealing that the sample mainly contain mesopores (2–50 nm). The formation of mesoporous structure is due to the volatilization of organics in the annealing process and aggregation of  $\text{NiCo}_2\text{O}_4$  crystallites. Based on the calculation of adsorption/desorption data, the surface area and pore diameter of this sample are  $134 \text{ m}^2 \text{ g}^{-1}$  and 3.75 nm, respectively.

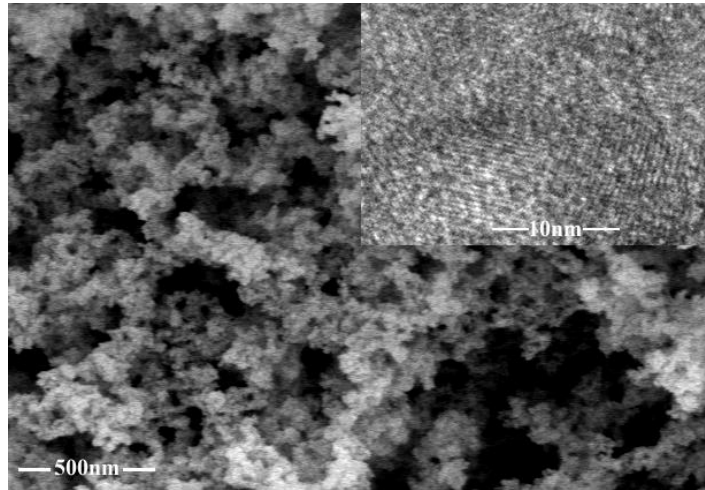


Fig. 2 SEM micrograph of the mesoporous  $\text{NiCo}_2\text{O}_4$  nanocomposite (inset: HRTEM image)

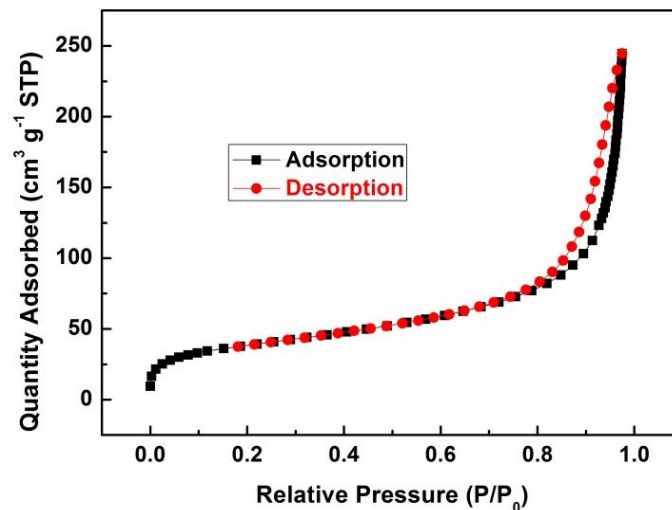


Fig. 3  $\text{N}_2$  adsorption and desorption isotherm of the mesoporous  $\text{NiCo}_2\text{O}_4$  nanocomposite

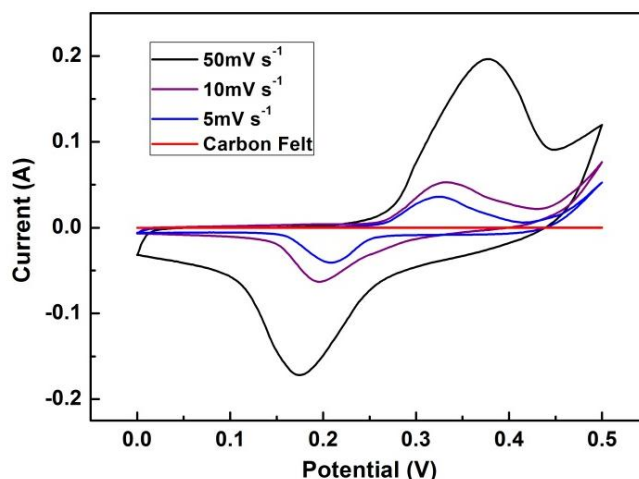


Fig. 4 CV curves of the mesoporous  $\text{NiCo}_2\text{O}_4$  electrode in a three-electrode system at different scan rate

Fig. 4 shows the CV curves of the as prepared mesoporous  $\text{NiCo}_2\text{O}_4$  nanocomposite measured at the scanning rates of 5, 10, and 50  $\text{mV s}^{-1}$  in the potential range of 0–0.5 V. A pair of redox peaks can be observed in those curves, indicating the strong Faraday's behavior of the as-obtained battery-type electrode. The CV curve areas also indicate that the as-obtained electrode possesses a significant specific capacity. In addition, the contribution of carbon felt can be negligible through the evaluation of the CV curve of carbon felt.

The GCD test is carried out at current densities of 1, 2, 5, 10, and 20  $\text{A g}^{-1}$  and within the potential range of 0–0.45V. The galvanostatic discharge curves of the mesoporous  $\text{NiCo}_2\text{O}_4$  electrode are shown in Fig. 5. The nonlinear variation of voltage as a function of time indicates the remarkable characteristic of the battery-type electrode. The maximum specific capacity of mesoporous  $\text{NiCo}_2\text{O}_4$  nanocomposite electrode is 392  $\text{C g}^{-1}$  at a current density of 1  $\text{A g}^{-1}$ , which is derived from the high specific surface area, mesoporous structure and good conductivity of  $\text{NiCo}_2\text{O}_4$  nanocomposite. As the current density increases to 20  $\text{A g}^{-1}$ , the capacity still keeps 263  $\text{C g}^{-1}$  (68.4% retention), suggesting that the electrode possesses excellent electrochemical performance for application in energy conversion.

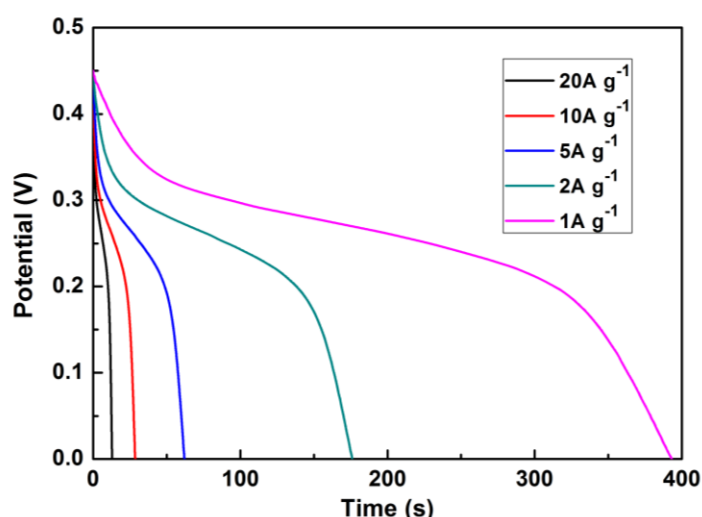


Fig. 5 Galvanostatic discharge curves of the mesoporous  $\text{NiCo}_2\text{O}_4$  electrode

## Summary

We have synthesized the mesoporous  $\text{NiCo}_2\text{O}_4$  nanocomposite through a xerogel route using propylene oxide as a gelation agent. The sample possesses a mesoporous structure and high specific surface area. The

results of electrochemical measurements indicate that the as obtained nanocomposite can deliver a maximum specific capacity of  $392 \text{ C g}^{-1}$  at a current density of  $1 \text{ A g}^{-1}$  based on the calculation of galvanostatic discharge, and these is a 68.4% retention at  $20 \text{ A g}^{-1}$ , promising for energy conversion devices in the future.

### Acknowledgement

We gratefully acknowledge the funding support by Laboratory of Precision Manufacturing Technology, CAEP (Grant No. KF15003).

### References

- [1] L. L. Zhang, X. Zhao, M. D. Stoller, Y. Zhu, H. Ji, S. Murali, Y. Wu, S. Perales, B. Cleverger, R. S. Ruoff, Highly conductive and porous activated reduced graphene oxide films for high-power supercapacitors, *Nano Letters*. 12 (2012) 1806-1812.
- [2] S. Han, D. Wu, S. Li, F. Zhang, X. Feng, Porous graphene materials for advanced Electrochemical energy storage and conversion devices, *Adv. Materials*. 26 (2014) 849-864.
- [3] K. Liang, X. Tang, W. Hu, High-performance three-dimensional nanoporous NiO film as a supercapacitor electrode, *Journal of Materials Chemistry* 22 (2012) 11062-11067.
- [4] A. D. Roberts, X. Li, H. Zhang, Porous carbon spheres and monoliths: morphology control, pore size tuning and their applications as Li-ion battery anode materials, *Chemical Society Reviews*, 43 (2014) 4341-4356.
- [5] L. Hu, Y. Deng, K. Liang, X. Liu, W. Hu, LaNiO<sub>3</sub>/NiO hollow nanofibers with mesoporous wall: a significant improvement in NiO electrodes for supercapacitors, *Journal of Solid State Electrochemistry* 19 (2015) 629-637.
- [6] X. Li, L. Jiang, C. Zhou, J. Liu, H. Zeng, Integrating large specific surface area and high conductivity in hydrogenated NiCo<sub>2</sub>O<sub>4</sub> double-shell hollow spheres to improve supercapacitors, *NPG Asia Materials*. 7 (2015) e165.
- [7] N. Wang, M. Yao, P. Zhao, Q. Zhang, W. Hu, Highly mesoporous structure nickel cobalt oxides with an ultra-high specific surface area for supercapacitor electrode materials, *Journal of Solid State Electrochemistry* 20 (2016) 1429-1434.
- [8] K. K. Naik, R. T. Khare, R. V. Gelamo, M. A. More, R. Thapa, D. J. Late, C. S. Rout, Enhanced electron field emission from NiCo<sub>2</sub>O<sub>4</sub> nanosheet arrays, *Materials Research Express* 2 (2015) 095011.
- [9] A. Jain, C. Xu, S. Jayaraman, R. Balasubramanian, J. Y. Lee, M. P. Srinivasan, Mesoporous activated carbons with enhanced porosity by optimal hydrothermal pre-treatment of biomass for supercapacitor applications, *Microporous and Mesoporous Materials* 218 (2015) 55-61.
- [10] A. B. Fuertes, M. Sevilla, Hierarchical microporous/mesoporous carbon nanosheets for high-performance supercapacitors, *ACS applied materials & interfaces* 7 (2015) 4344-4353.
- [11] A. K. Mondal, D. Su, S. Chen, K. Kretschmer, X. Xie, H.-J. Ahn, G. Wang, A microwave synthesis of mesoporous NiCo<sub>2</sub>O<sub>4</sub> nanosheets as electrode materials for lithium-ion batteries and supercapacitors, *Chemphyschem*. 16 (2015) 169-175.
- [12] Y. Li, L. Zou, J. Li, K. Guo, X. Dong, X. Li, X. Xue, H. Zhang, H. Yang, Synthesis of ordered mesoporous NiCo<sub>2</sub>O<sub>4</sub> via hard template and its application as bifunctional electrocatalyst for Li-O<sub>2</sub> batteries, *Electrochimica Acta*. 129 (2014) 14-20.

- [13] M. U. A. Prathap, C. Wei, S. Sun, Z. J. Xu, A new insight into electrochemical detection of eugenol by hierarchical sheaf-like mesoporous NiCo<sub>2</sub>O<sub>4</sub>, *Nano Research* 8 (2015) 2636-2645.
- [14] Y Liu, N Wang, C Yang, W Hu, Sol-gel synthesis of nanoporous NiCo<sub>2</sub>O<sub>4</sub> thin films on ITO glass as high-performance supercapacitor electrodes, *Ceramics International* 42 (2016) 11411-11416.
- [15] H. Y. Fu, Z. Y. Wang, Y. H. Li, Y. F. Zhang, Electrochemical deposition of mesoporous NiCo<sub>2</sub>O<sub>4</sub> nanosheets on Ni foam as high-performance electrodes for supercapacitors, *Materials Research Innovations* 19 (2015) 255-259.
- [16] J. Rouquerol, D. Avnir, C. W. Fairbridge, D. H. Everett, J. M. Haynes, N. Pernicone, J. D. F. Ramsay, K. S. W. Sing, K. K. Unger, Recommendations for the characterization of porous solids, *Pure and Applied Chemistry* 66 (1994) 1739-1758.